Trigonal NHC bis-pyridyl silver complexes a beacon of light in the darkness of LEC?

Ginevra Giobbio,[a,b] Lucie Greffier,[c] Sophia Lipinski,[b] Anaïs Montrieul,[a] Jean-François Lohier,[a] Mathieu Linares,[c] Rubén D. Costa[,b] and Sylvain Gaillard*[,a]*

[a] Dr. G. Giobbio, Anaïs Montrieul, Dr Jean-François Lohier and Dr. S. Gaillard
Normandie University, ENSICAEN, UNICAEN, CNRS, LCMT, 14000 Caen, France. e-mail: sylvain.gaillard@ensicaen.fr

[b] Dr. G. Giobbio and Prof. Dr. R. D. Costa
Chair of Biogenic Functional Materials, Technical University of Munich, Campus Straubing for Biotechnology and Sustainability, Schulgasse 22, 94315 Straubing, Germany. e-mail: ruben.costa@tum.de

[c] Lucie Greffier
Division of Theoretical Chemistry and Biology, School of Engineering Sciences in Chemistry, Biotechnology and Health, KTH Royal Institute of Technology, SE-100 44 Stockholm, Sweden

[d] Dr. M. Linares
PDC Centre for High Performance Computing, EECS, KTH Royal Institute of Technology, Stockholm, Sweden

Table of Content

Theoretical details

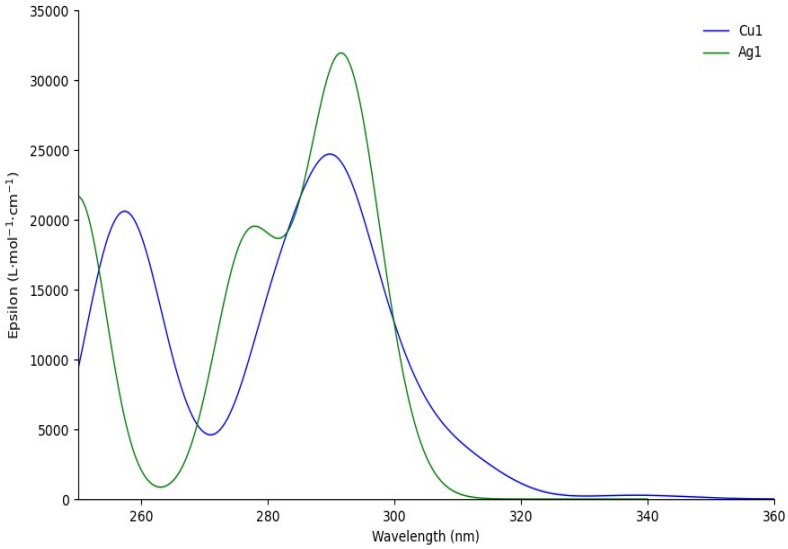

Figure S1. Theoretical UV-visible absorption spectra of **1** (green curve) and **2** (blue curve).

Table S1. Wavelengths (in eV and nm) for the calculated excited states and their oscillation strength for **1**. The excited states with a star (*) are those with the highest oscillation forces.

	λ (nm)	λ (eV)	Oscillator Strength
State 1*	281	4.41	0.2327
State 2	277	4.48	0.0029
State 3*	277	4.48	0.135
State 4	266	4.66	0.0006
State 5*	251	4.94	0.0776
State 6*	249	4.97	0.0813
State 7	244	5.08	0.0022
State 8	244	5.08	0.0016
State 9	242	5.11	0.0073
State 10	242	5.12	0.0045
State 11	242	5.13	0.0081
State 12	239	5.18	0.001

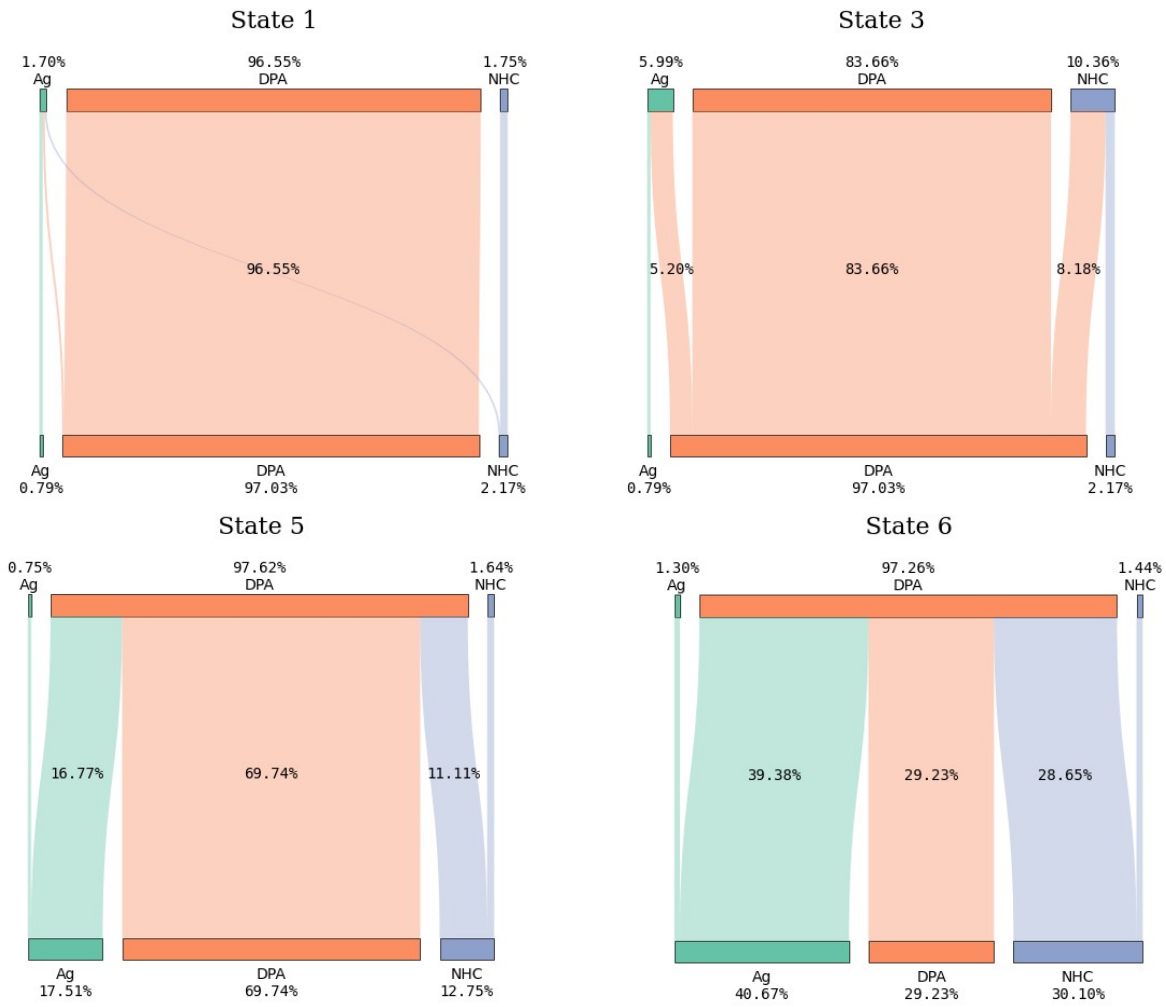

Figure S2. Calculated natural transition orbitals (NTOs) for **1**. The excited state 6 and 7 corresponded to the first band of the calculated UV-visble spectrum (250-275 nm, Figure S1) and excited states 1 and 3 to the second band of the calculated UV-visible spectrum (280-360 nm, Figure S1).

Table S2. Wavelengths (in eV and nm) for the calculated excited states and their oscillation strength for **2**. The excited states with a star (*) are those with the highest oscillation forces.

	λ (nm)	λ (eV)	Oscillator Strength
State 1	338	3.66	0.0021
State 2	328	3.78	0
State 3	311	3.98	0.0179
State 4*	300	4.13	0.0448
State 5 *	291	4.26	0.1298
State 6	289	4.30	0.0208
State 7*	281	4.41	0.0817
State 8	281	4.42	0.0031
State 9	281	4.42	0.0085
State 10	267	4.64	0.0083
State 11	262	4.73	0
State 12	260	4.77	0.0407
State 13*	260	4.77	0.0535
State 14	255	4.86	0.0045
State 15	255	4.87	0.0021
State 16*	255	4.87	0.0381
State 17*	254	4.88	0.0432
State 18	250	4.97	0.004
State 19	249	4.98	0.0002
State 20	248	4.99	0.0041

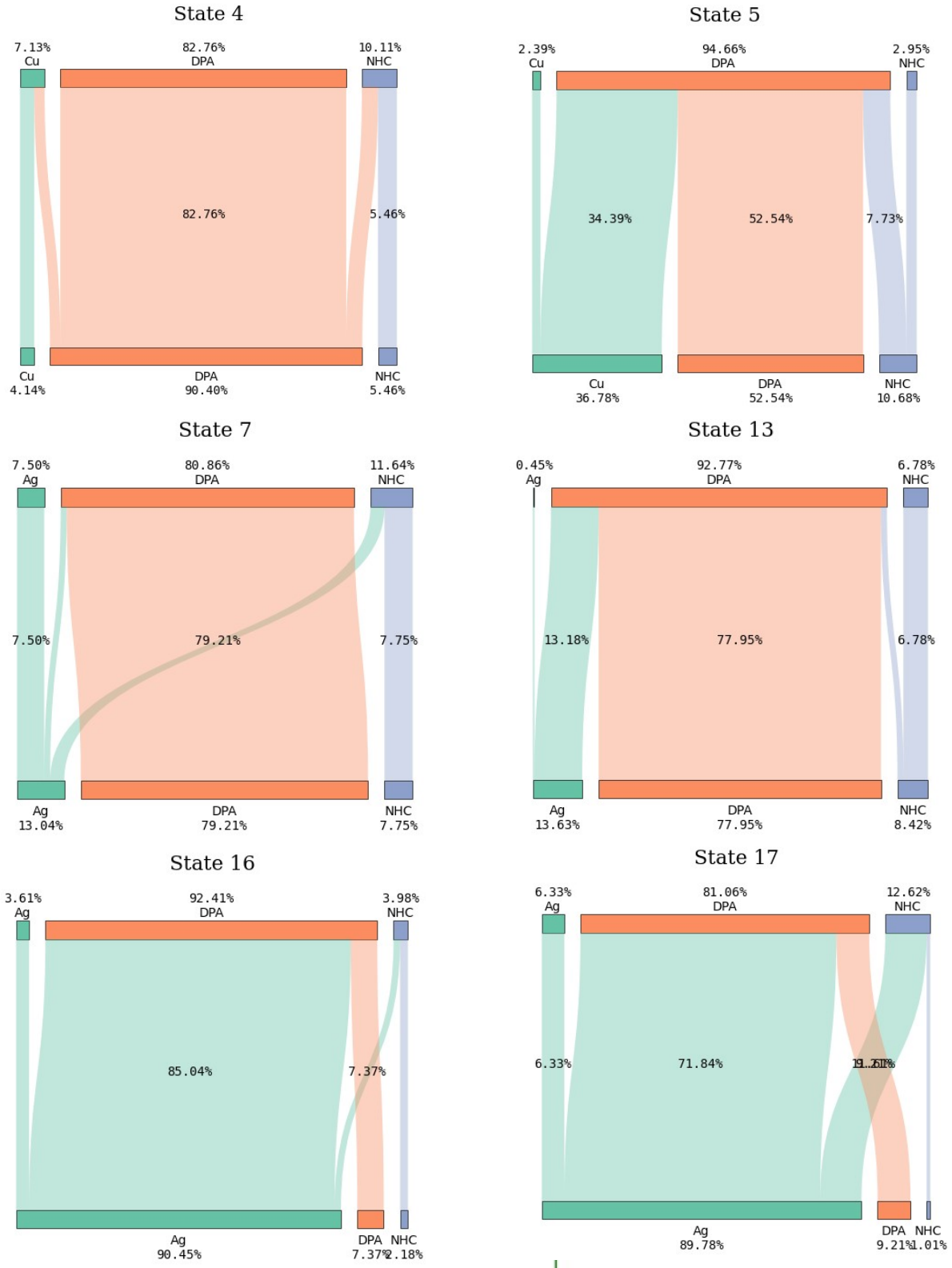

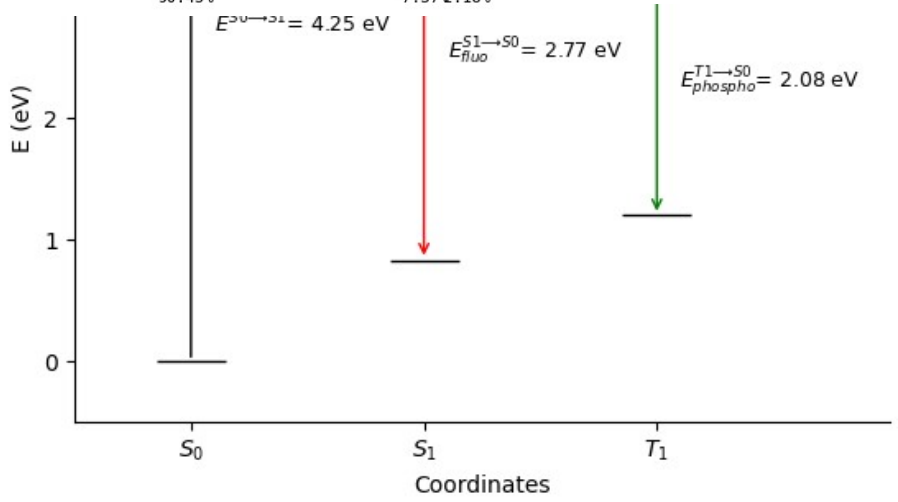

Figure S3. Calculated natural tra
of the calculated UV-visble spec
calculated UV-visible spectrum

Figure S4. Jablonski diagram of **1**. The black dashes correspond to the ground state (S0), the red to the first singlet excited state(S1) and the green to the first triplet excited state (T1).

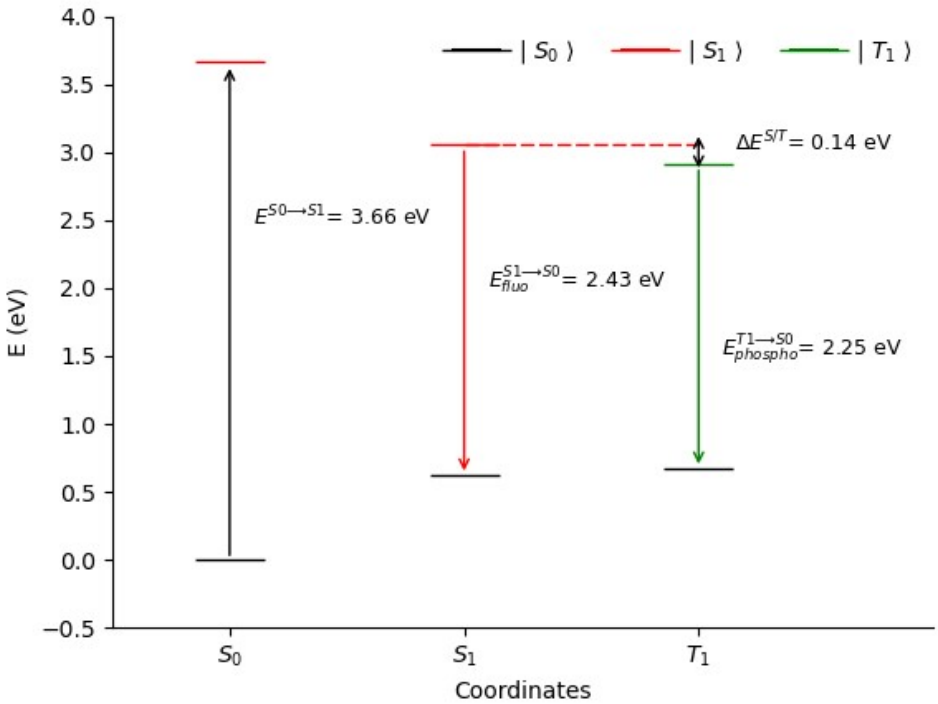

Figure S5. Jablonski diagram of
excited state (S1) and the green t

Synthesis of complex **1**

The [Ag(IPr)Cl] complex (1 eq.) and 3,3'-dimethyl-2,2'-dipyridylamine ($^{3\text{-Me}}$dpa) (1.05 eq.) were dissolved in degassed absolute ethanol in a flame-dried Schlenk tube under an argon atmosphere. The mixture was heated to reflux for 1 hour. After cooling to room temperature, a saturated aqueous solution of KPF_6 was introduced, resulting in the formation of a white precipitate. The solid was

subsequently washed with water and diethyl ether before being dried under vacuum.

[Ag(IPr)($^{3\text{-Me}}$dpa)][PF_6] – **1**: The white precipitate have been dissolved in the minimum amount of dichloromethane. The pure complex has been isolated as white needle-like crystals by slow diffusion of diethyl ether in the DCM solution (y = 30 %). ^{1}H NMR ($CDCl_3$, 500 MHz): δ 1.12 (d, *J* = 6.9 Hz, 12H), 1.26 (d, *J* = 6.9 Hz, 12H), 2.30 (s, 6H), 2.57 (sept, *J* = 6.9 Hz, 4H), 6.01 (s, 2H), 6.47 (t, *J* = 7.0 Hz, 2H), 6.57 (br s, 1H), 7.39 (d, *J* = 1.8 Hz, 2H), 7.40 (d, *J* = 7.9 Hz, 4H), 7.45 (d, *J* = 7.3 Hz, 2H), 7.67 (t, *J* = 7.8 Hz, 2H) ppm. ^{13}C NMR ($CDCl_3$, 151 MHz): δ 17.5 (s), 23.9 (s), 25.0 (s), 29.0 (s), 117.1 (s), 121.8 (s), 124.2 (d, $J_{Ag\text{-}C}$ = 7.7 Hz, C imidazole), 124.8 (s), 130.8 (s), 135.7 (s), 140.3 (s), 140.2 (s), 146.4 (s), 146.9 (s), 152.5 (s), 185.7 (d, *J* (^{13}C-^{107}Ag) = 250.3 Hz), 185.7 (d, *J* (^{13}C-^{109}Ag) = 291.1 Hz) ppm. ^{31}P NMR ($CDCl_3$, 202 MHz): δ -144.36 (sept, *J* (^{31}P-^{19}F) = 710.7 Hz, 1P) ppm. ^{19}F NMR ($CDCl_3$, 471 MHz): δ -73.71 (d, *J* (^{19}F-^{31}P) = 713.0 Hz, 6F) ppm. HRMS (ESI): m/z calcd for $C_{39}H_{49}N_5Ag[M\text{-}PF_6]^+$ 694.3039, found 694.3034. IR 3435.5, 2926.5, 1738, 1590, 1462, 1117, 1004, 836, 557 cm^{-1}.

NMR spectroscopy copies

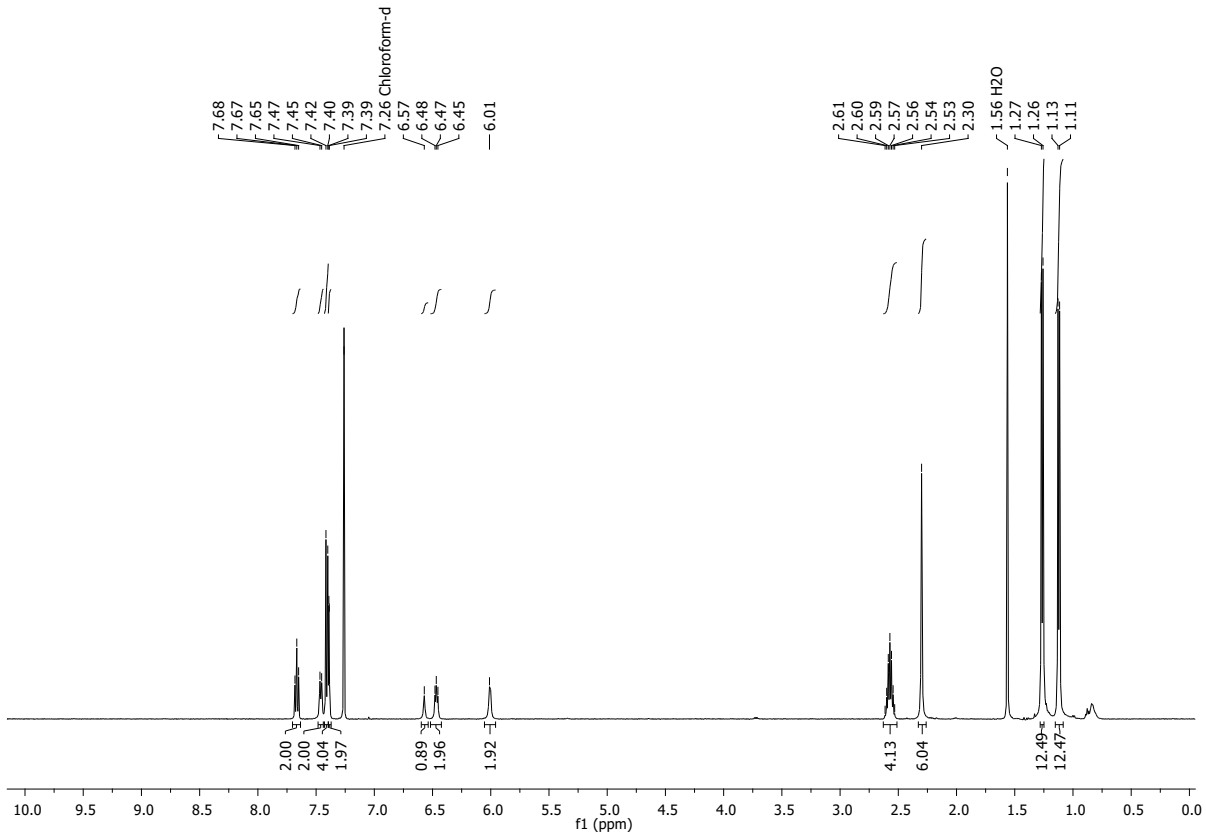

Figure S6. ^{1}H NMR ($CDCl_3$, 500 MHz) of [Ag(IPr)($^{3\text{-Me}}$dpa)][PF_6] (**1**).

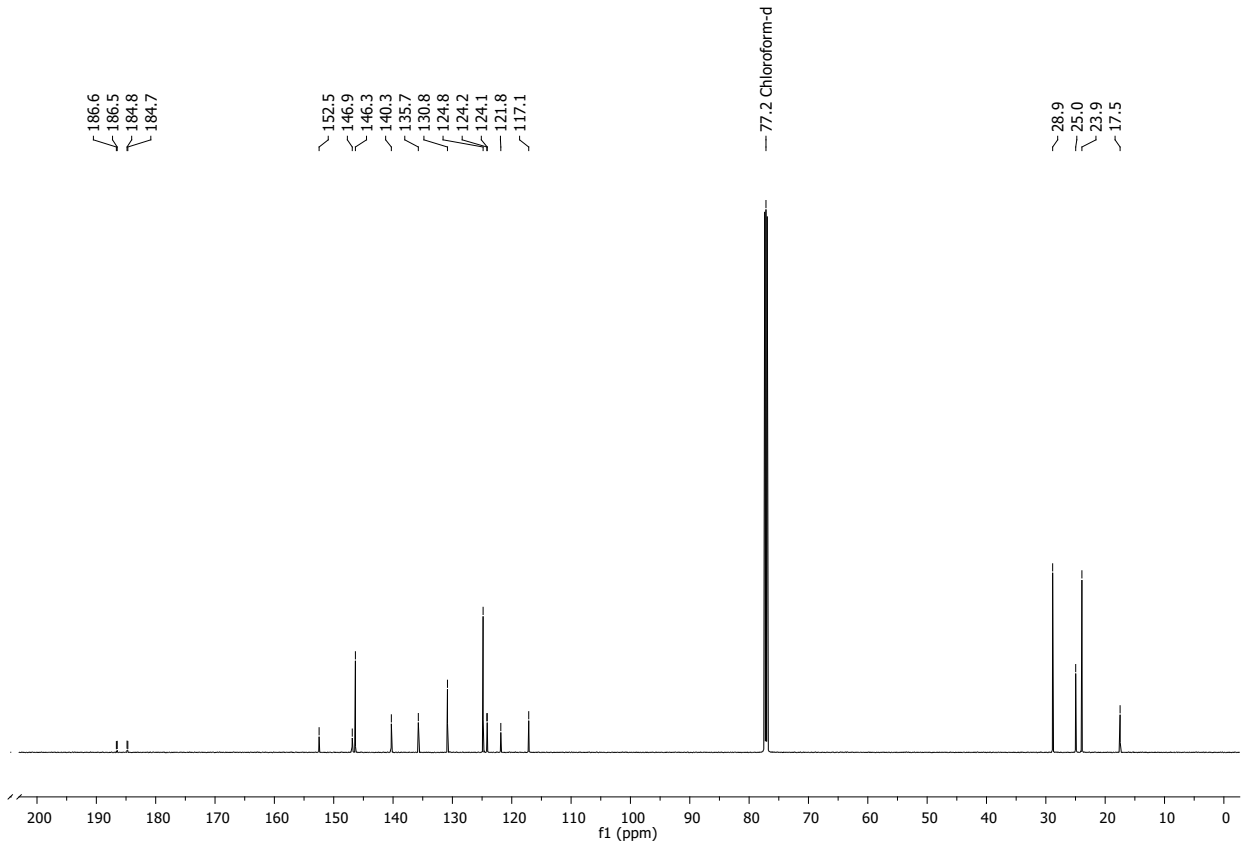

Figure S7. ^{13}C NMR ($CDCl_3$, 151 MHz) of [Ag(IPr)($^{3\text{-Me}}$dpa)][PF_6] (**1**).

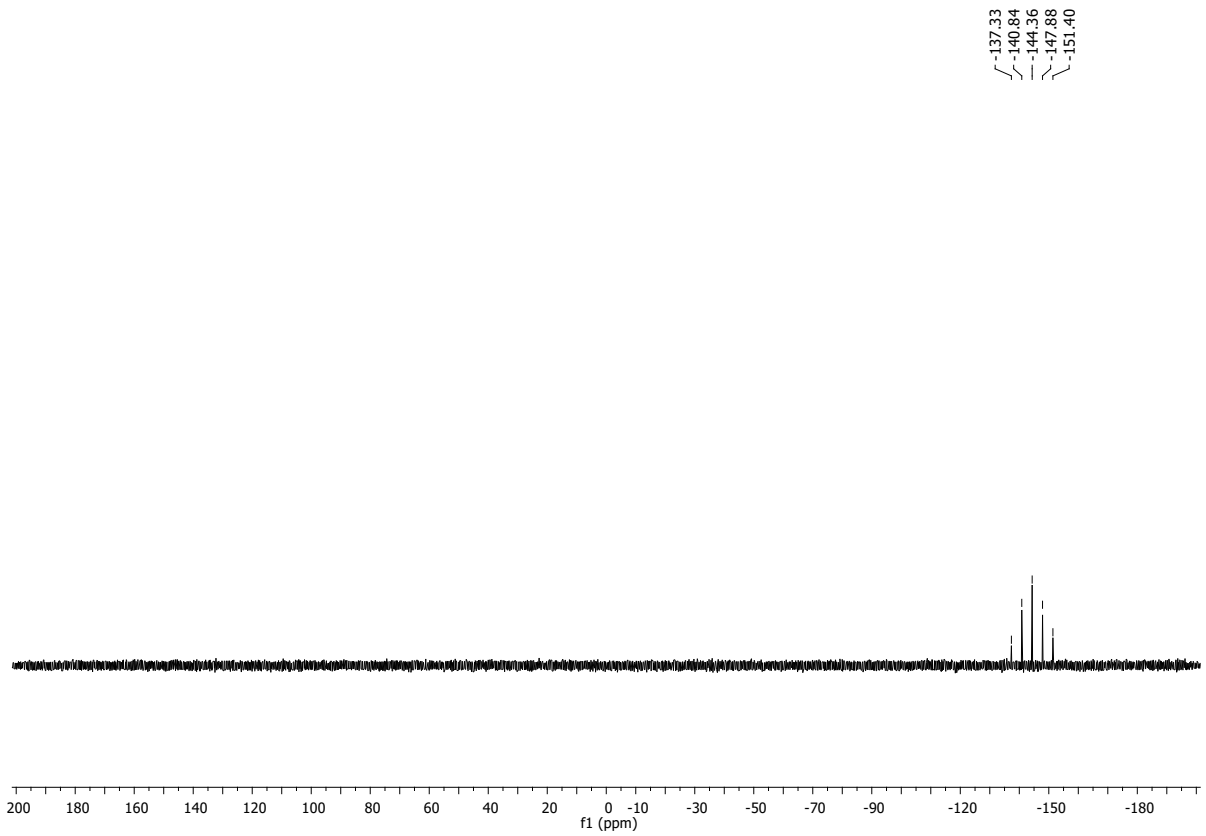

Figure S8. ^{31}P NMR ($CDCl_3$, 202 MHz) of [Ag(IPr)($^{3\text{-Me}}$dpa)][PF_6] (**1**).

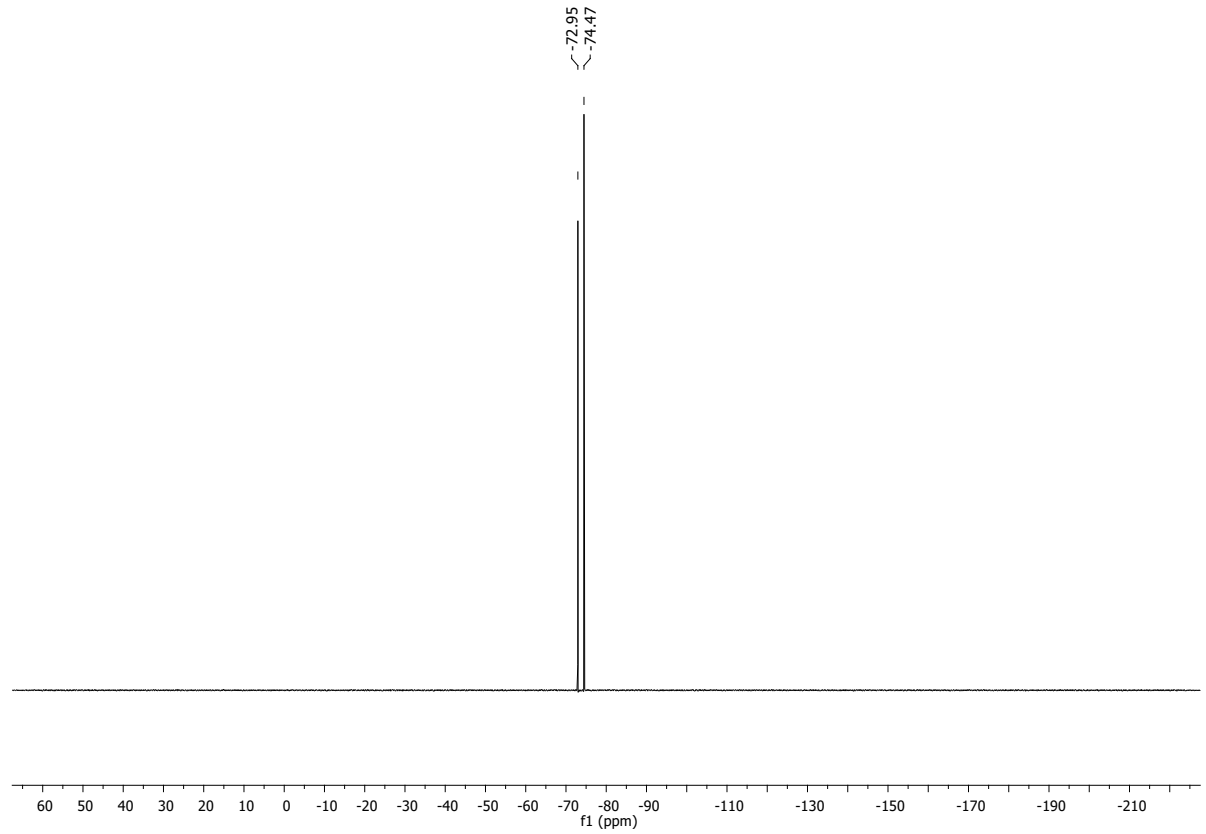

Figure S9. ^{19}F NMR ($CDCl_3$, 471 MHz) of [Ag(IPr)($^{3\text{-Me}}$dpa)][PF_6] (**1**).

X-Ray diffraction details

Table S3. Crystallographic data of complex **1**.

	1
Formula	$C_{39}H_{49}AgF_6N_5P$
M/g·mol^{-1}	840.67
Crystal system	orthorhombic
Space group	*P* bca
a/ Å	15.8119(5)
b/ Å	17.8148(5)
c/ Å	28.1724(9)
α/ °	90
β/ °	90
γ/ °	90
V/ Å^3	7935.8(4)
Z	8
μ/ mm^{-1}	0.611
ρcalcd/ g·cm^{-3}	1.407
λ (Mo K_α)/ mm^{-1}	0.71073
T/ K	123(2)
N° of reflections	11620
N° of unique reflection	9118
R_{int}	0.072503
R1, wR_2 (I > 2σ(I))	0.031473
R1, wR_2 (all data)	0.048141
GOF	1.01949

Photophysical measurements of thin films

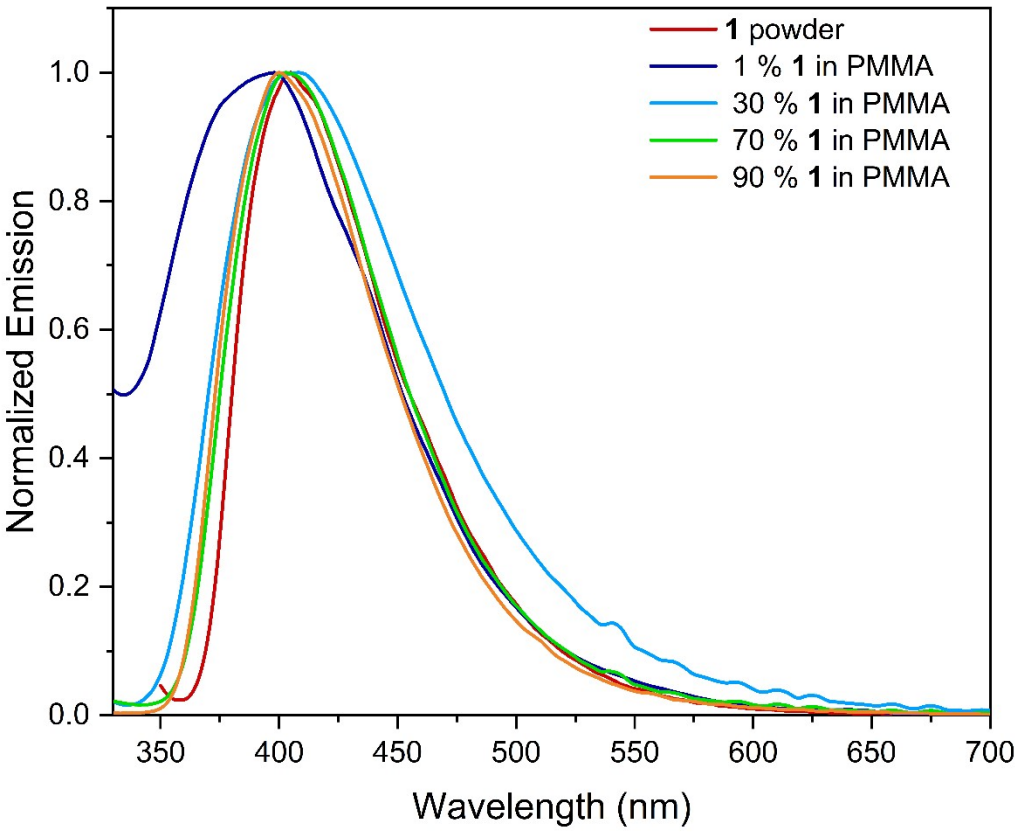

Figure S10. Emission spectra of **1** in thin film.

Cyclic Voltammetry

General considerations*:* The cyclic voltammetry experiments were performed at room temperature with Autolab PGSTAT101 (Metrohm) potentiostat unit (Nova 2.1 software package). The standard three-electrodes configuration cell was equipped using a glassy-carbon as working electrode, platinum wire and Ag/AgCl as auxiliary and reference electrode, respectively. The measurement is performed at a step potential of 0.00244 V and scan rate of 0.0.005 V/s. The analysis was performed on a solution of [Ag(IPr)($^{3\text{-Me}}$dpa)][PF_6] (**1**) in anhydrous and degassed n-Bu_4NPF_6 (0.1 M) in THF. The system was calibrated with a solution of ferrocene (Fc/Fc^+ = 0.46 V).

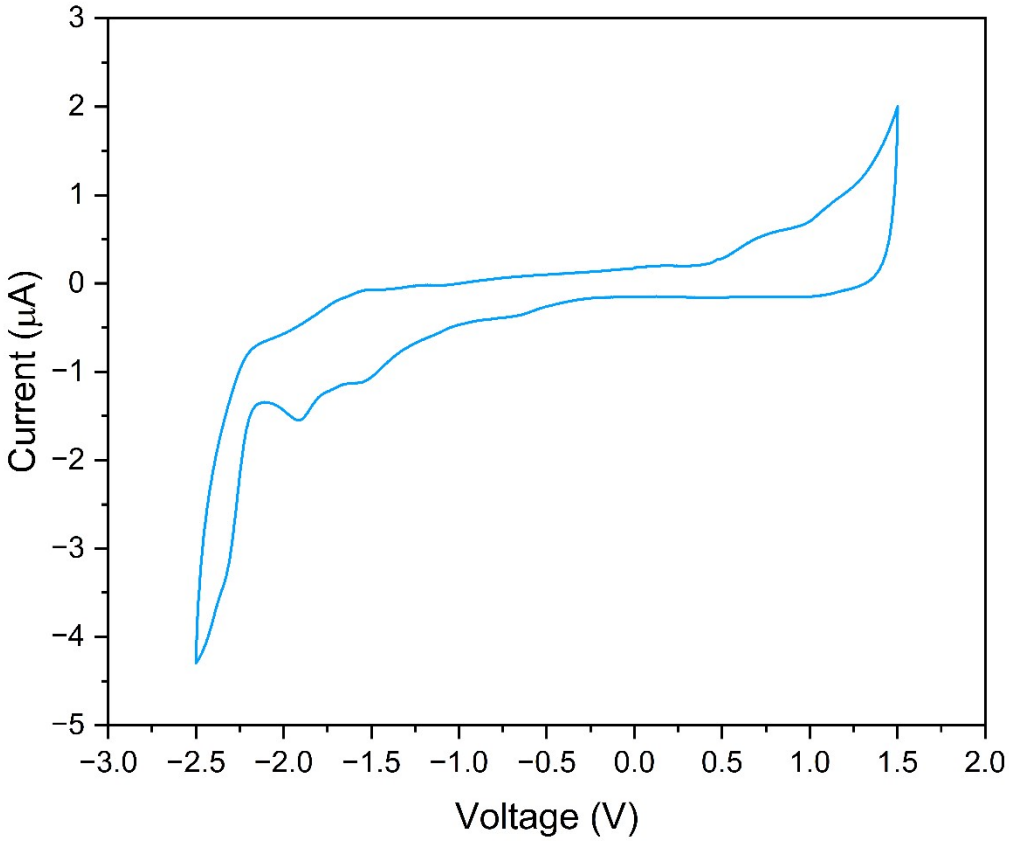

Figure S11. Cyclic voltammogram of [Ag(IPr)($^{3\text{-Me}}$dpa)][PF_6] (**1**) in anhydrous and degassed n-Bu_4NPF_6 (0.1 M) in THF with a scan rate of 0.005 V/s.

Electrochemical Impedance Spectroscopy

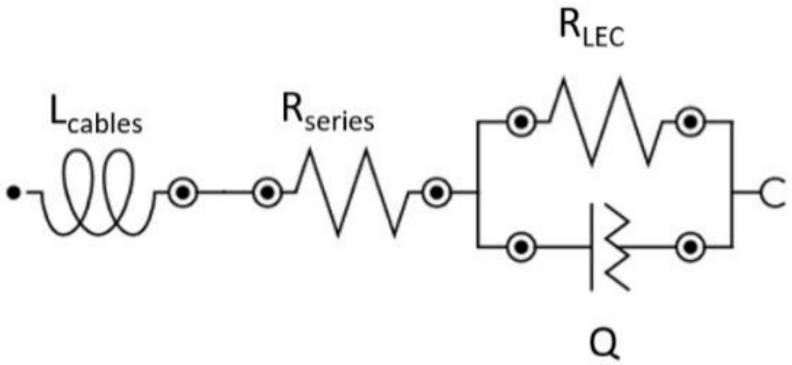

Figure S12. Simplified circuit model with electrical resistance (R_{LEC}) and Constant Phase Element (Q) used for static EIS assays. A series resistor (R_{series}) and inductor elements for the cables (L_{cables}) were also included.[1,2]

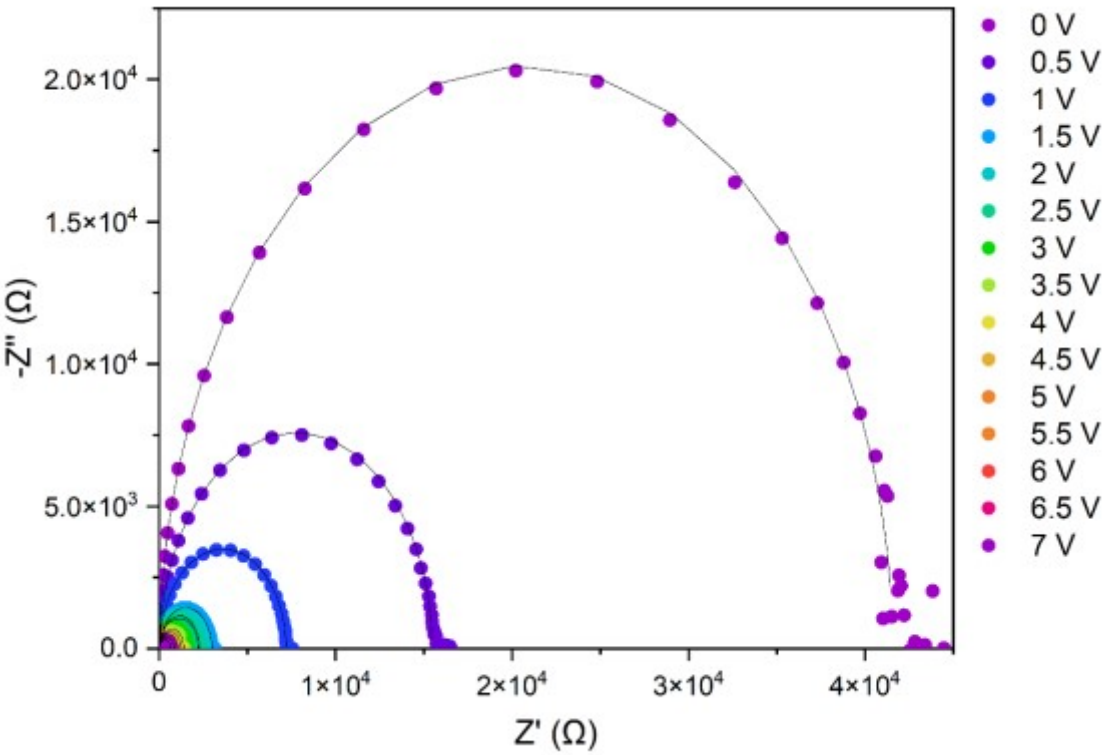

Figure S13. Nyquist plot of [Ag(IPr)($^{3\text{-Me}}$dpa)][PF_6] (**1**) – based fresh device.

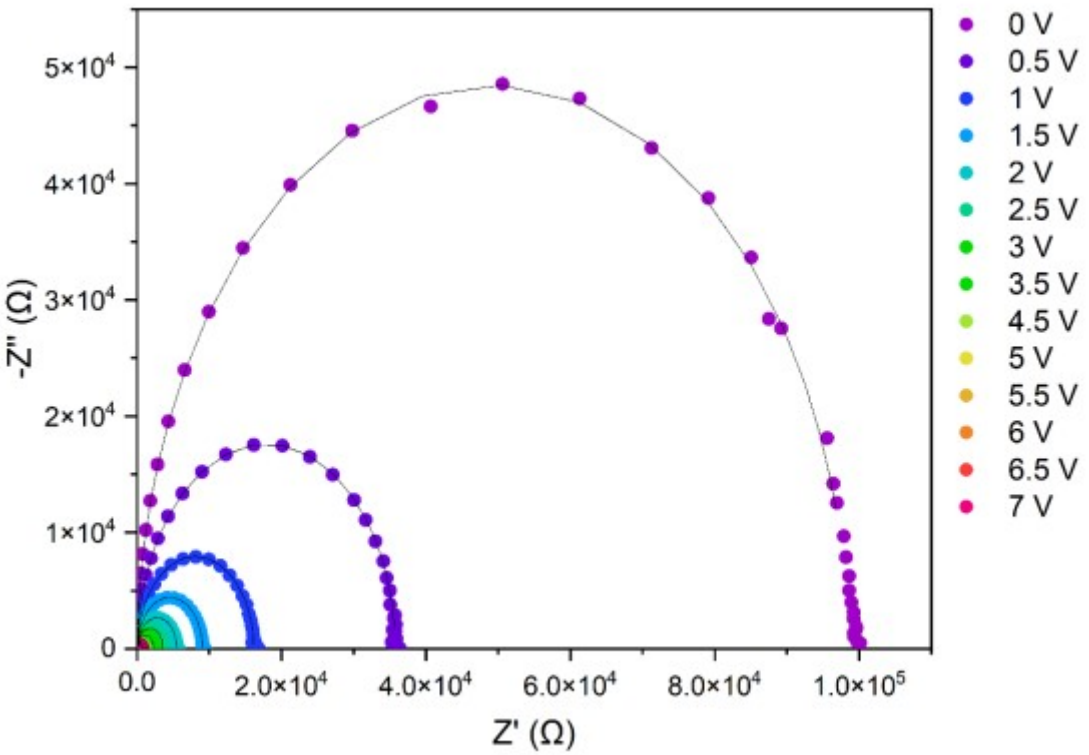

Figure S14. Nyquist plot of [Ag(IPr)($^{3\text{-Me}}$dpa)][PF_6] (**1**) – based used device.

References

1 S.B. Meier, D. Hartmann, A. Winnacker and W. Sarfert, *J. Appl. Phys.*, 2014, **116**, 104504.

2 S. B. Meier, D. Hartmann, D. Tordera, H. J. Bolink, A. Winnacker and W.Sarfert, *Phys.Chem.Chem.Phys*., 2012, **14**, 10886